Nuclear activation as a high dynamic range diagnostic of laser–plasma interactions

R.J. Clarke[a],*, P.T. Simpson[b], S. Kar[b], J.S. Green[a], C. Bellei[c], D.C. Carroll[d], B. Dromey[b], S. Kneip[c], K. Markey[b], P. McKenna[d], W. Murphy[e], S. Nagel[c], L. Willingale[c], M. Zepf[b]

[a]STFC Rutherford Appleton Laboratory, Room 2-79, Building R1, Chilton, Didcot, Oxfordshire OX11 OQX, UK
[b]Department of Physics and Astronomy, Queens University Belfast, Belfast BT7 1NN, Northern Ireland, UK
[c]Department of Physics, Imperial College London, Blackett Laboratory, London SW7 2BZ, UK
[d]SUPA, Department of Physics, University of Strathclyde, Glasgow G4 0NG, UK
[e]Department of Physics, University of Oxford, Oxfordshire OX1 3QR, UK

Abstract

Proton imaging has become a common diagnostic technique for use in laser–plasma research experiments due to their ability to diagnose electric field effects and to resolve small density differences caused through shock effects. These interactions are highly dependent on the use of radiochromic film (RCF) as a detection system for the particle probe, and produces very high-resolution images. However, saturation effects, and in many cases, damage to the film limits the usefulness of this technique for high-flux particle probing. This paper outlines the use of a new technique using contact radiography of (p,n)-generated isotopes in activation samples to produce high dynamic range 2D images with high spatial resolution and extremely high dynamic range, whilst maintaining both energy resolution and absolute flux measurements.

The field of laser–plasma interactions for the optimisation (and use) of ion acceleration and nuclear interactions is still greatly expanding, with goals such as the generation or selection of mono-energetic ions [1–5], and the generation of high-energy protons for particle probing or proton radiography [6]. Most of this research uses activation techniques [7,8] or track detectors (CR39) coupled to Thomson spectrometers [9,10] for determination of proton energies. The observation of 2D properties such as that required for particle probing has been limited to the use of track detectors and radiochromic film (RCF), the latter being the only technique to date that has provided the high resolution required for techniques such as proton imaging. The use of activated materials for this purpose has

previously been attempted to observe global beam structures [11], and has shown positive results, but no attempts to observe fine structures as required for particle probing techniques have been performed until now.

The Vulcan Petawatt facility at Rutherford Appleton Laboratory [12] was used to generate high-energy, high-flux proton beams, for the investigation of proton divergence with varying target parameters. As part of these measurements, copper meshes were used to generate a grid pattern in the proton beam, used as a direct map for measuring divergence changes within the proton beam. The primary detector used was RCF (HD-810 and HS), providing a 2-D image of the emitted proton beam. Silver and copper foils were used for energy filtering within the RCF stack, with the whole stack positioned at ~50 mm from the interaction point. The silver foils were used to reduce the observed activity in order to minimise the

---

exposure to the radioactive material. The copper foils enabled absolute proton flux measurements to be made through the ^{63}Cu (p,n) ^{63}Zn reaction, decaying through 511 keV β^+ emission, and measured using NaI coincidence detectors. The energy filtering foils were removed from the RCF stack and, in the case of the copper foils after measurements with the co-incidence system, were placed onto Fuji image plates [13], and left to be exposed to the radiation emitted from the decaying isotopes. The silver foils, producing 93 keV photons from the ^{107}Ag (p,n) ^{107}Cd reaction with a half-life of 6.5 h, were left for an overnight exposure, whereas the copper foils were left for approximately 1 h, as the generated ^{63}Zn positron emitting isotope has a half-life of just over 38 min. The image plates were scanned and the resultant images compared with that of the RCF images, as shown in Fig. 1. It should be noted that although the foil and RCF positions within the stack are positioned together, they do not sample the same energy slice. This is due to the threshold energy for generating a (p,n) reaction being typically around 4–5 MeV, whereas the RCF responds directly to the incoming radiation dose.

On comparing the 5 MeV images in Fig. 1, taken from silver activation foils and RCF, it is clear that the RCF is highly saturated, with little details observable within the central region. These structures are however still visible within the contact radiograph as no saturation can occur within the samples with currently achievable proton fluxes. Any saturation of the image plate can easily be removed by a second scanning of the image plate after a short wipe period (controlled exposure to white light). Typically, a duration of between 10 and 30 s is used. Alternatively, a second exposure can be made from the activated foils once the activity has further decayed. These simple techniques can expand the 16 bit dynamic range of the image plate by at least several orders of magnitude in signal levels. These are the techniques that allow access to regions of extremely high flux with the contact radiography method, where RCF currently fails. The image quality and contrast observed is a function of the exposure duration and activity of the foils. The optimum conditions as a function of activity, half-life and exposure times require further investigation. For long exposures the image plate should be shielded to reduce the build-up of cosmic rays, which reduce the signal-to-noise ratio.

The higher energy bins (14 and 18 MeV) in Fig. 1 from the same shot show good correspondence between the images for both the RCF and contact radiography. These images clearly show the mesh structure imprinted on the proton beam by a copper grid placed behind the target for proton beam divergence measurements. Contact radiographs taken from copper foils are shown in Fig. 2, with the exposure being performed after co-incidence counting. These radiographs are taken from a selection of shots and clearly show that the contact radiographs can produce high-resolution images.

Linear profiles of the right image in Fig. 2 are compared to those of the corresponding RCF image for the same proton energy. The location of the profiles in each image is shown in Fig. 3. The RCF was scanned using a high-resolution scanner. The profile results, performed on the original 16 bit images rather than the 8 bit processed image, shown throughout this paper are plotted in Fig. 4. The image plate profiles are shown in linear photo-stimulated luminescence (PSL), and the scanned RCF data in adjusted counts. The mesh structure is visible in both images and profiles. For these scans, the image plate scanner was used at it has a maximum resolution of 50 μm. The optical scanner used for scanning the RCF used a resolution of 300 dpi (optical), producing a pixel size of ~85 μm. The observed mesh features fall at a separation of 2.3 mm, with an average line thickness of 0.4 mm, well above the resolution limits of both the image plate and RCF optical scanner. The mesh through which the proton beam passed had a line period of 124.8 μm (~200 lines/in.) with a line thickness of 30.8 μm, measured using a high-resolution automated microscope. It is clear that features on the order of the mesh thickness (~30 μm) are visible in the contact radiographs with the magnification used. The visibility
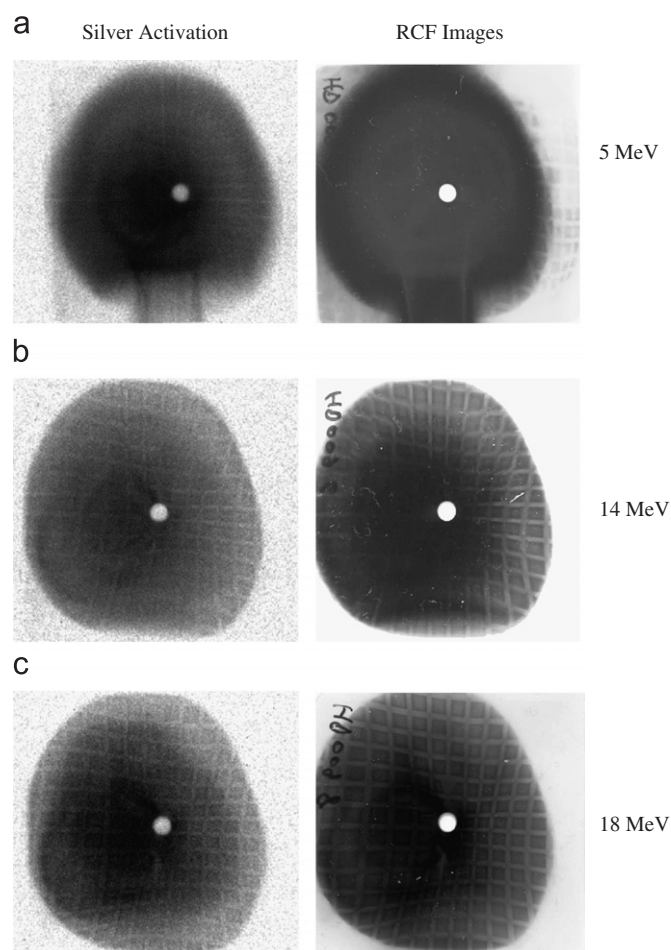

Fig. 1. Comparative images of radiochromic film (right) and the results of contact radiography with adjoining silver foils (left), created from a proton beam emitted from a thin foil laser–matter interaction. The two-directional mesh structure used for proton beam divergence measurements can clearly be observed. Images have been contrast enhanced for clarity.
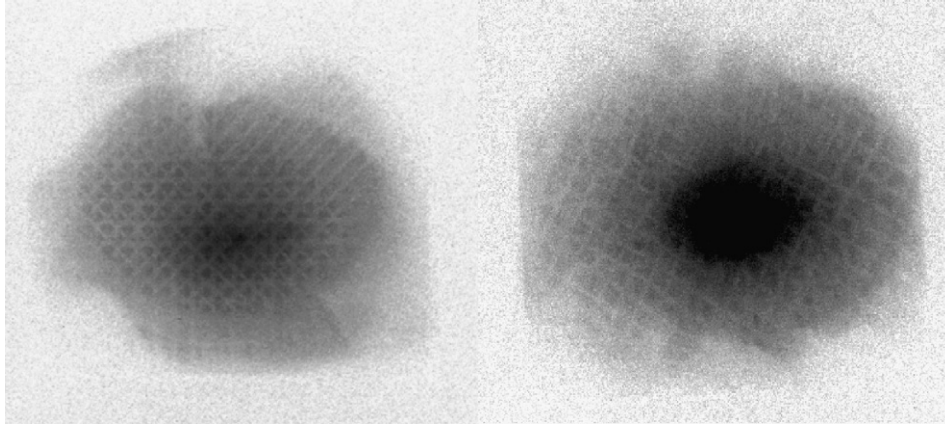
Fig. 2. Contact radiograph images from Cu activation foils. A three-directional mesh used for proton divergence measurements is clearly observable within the emitted proton beam structure.
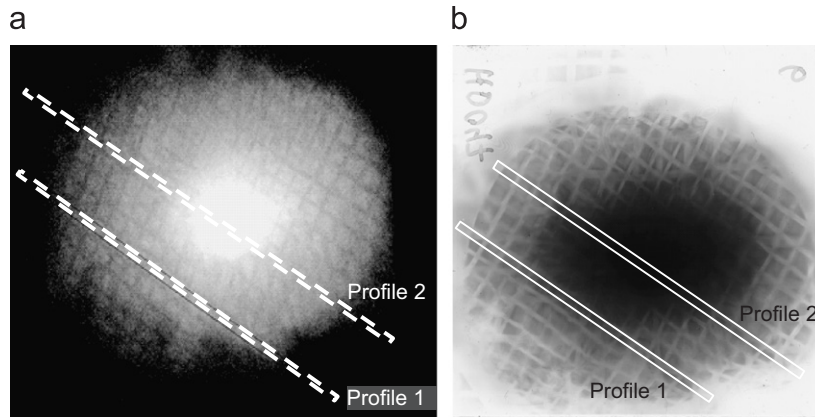

Fig. 3. Comparison of copper activation and RCF images used for profiling. (a) Contact radiograph of copper sample and (b) the corresponding RCF image.

(Eq. (1)) of fringes around the 24 mm position in Fig. 4(a) is 0.07, using an average for the peak height background around the peaks.

$$V = \frac{\text{Max} - \text{Min}}{\text{Max} + \text{Min}}. \tag{1}$$

It can be seen from the profile data in Fig. 4 that there is little difference in the visibility of the mesh structure between the radiograph and the RCF at the offset position. Profiling through the centre of the image, however, shows similar results in the wings. However, in the central region it is clear that the features in the high signal area are not visible in the RCF due to saturation effects. The fringes in the high signal region of the contact radiographs are still visible, highlighting the dynamic range capabilities.

This technique is not limited only to proton detection. Measurements of (γ, mn) reactions for detecting high-energy (>15 MeV) photons have been used for radiological measurements [14–16], and have also been used to map the divergence of high-energy photons through the use of interlaced samples and separate measurements of each sample [17,18]. These techniques can be replaced with simple radiographs, allowing both flux and divergence measurements to be made simultaneously.

Further study is planned, using this technique as a particle probe, for laser–plasma interactions. Typically, the proton energies (and hence depth in the detector stack) are used to map the temporal properties of the probed interaction. The wide cross-section peak (typically tens of MeV) could generate a "blurring" of images as multiple images from multiple proton energies are overlapped. If this is so, this technique would be best suited for low-energy proton probing, where proton energies lie close to the cross-section threshold.

In conclusion, the use of contact radiography appears to be a viable alternative to the use of RCF for low repetition, high signal particle beams, counteracting saturation effects whilst maintaining a high resolution. The selection of particles for imaging can be made using different activation materials, provided the particle energy is above the threshold values for the nuclear reactions required. This technique also permits the ability to perform absolute particle flux measurements through already established nuclear techniques.
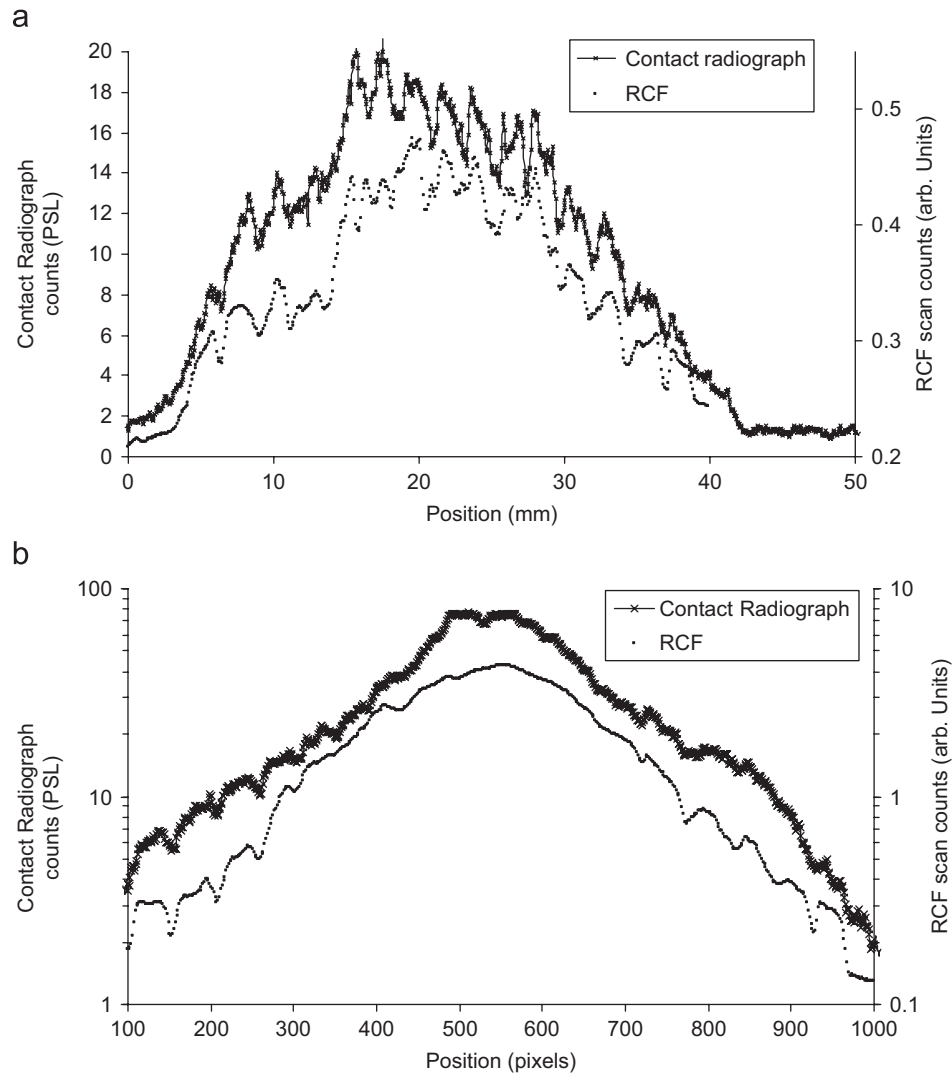
Fig. 4. Profile data taken from Fig. 3 for the contact radiograph and RCF: (a) Offset position (profile 1) and (b) intersecting the brightest region through the centre (profile 2).

References

[1] W. Lou, et al., Med. Phys. 32 (2005) 794.
[2] K. Ledingham, Nat. Phys. 2 (2006) 11.
[3] J. Fuchs, et al., Nat. Phys. 2 (2006) 48.
[4] T. Toncian, et al., Science 312 (2006) 410.
[5] L. Robson, et al., Nat. Phys. 3 (2007) 58.
[6] M. Borghesi, et al., Plasma Phys. Controlled Fusion 43 (2001) 267.
[7] M. Zepf, et al., Phys. Plasmas 8 (2001) 2323.
[8] I. Spencer, et al., Nucl. Instr. and Meth. in Phys. Res. B 183 (2001) 449.
[9] J.J. Thomson, Philos. Mag. 21 (1911) 225.
[10] E.L. Clark, et al., Phys. Rev. Lett. 85 (2000) 1654.
[11] P. McKenna, et al., Laser-driven ion acceleration and nuclear activation, in: Lasers and Nuclei, vol. 694, pp. 91–107, ISBN: 978-3-540-30271-1.
[12] C.N. Danson, et al., J. Nucl. Fusion 44 (2004) S239.
[13] Y. Amemiya, J. Miyahara, Nature 336 (1988) 89.
[14] T.W. Philips, et al., Rev. Sci. Instrum. 70 (1999) 1213.
[15] K.W.D. Ledingham, et al., Phys. Rev. Lett. 84 (2000) 899.
[16] R.J. Clarke, et al., J. Radiol. Prot. 26 (2006) 277.
[17] M.I.K. Santala, et al., Phys. Rev. Lett. 84 (2000) 1459.
[18] S.P. Hatchett, et al., Phys. Plasmas 7 (2000) 2076.